Electron Scattering from the Deuteron*

JOHN A. MCINTYRE
High-Energy Physics Laboratory, Stanford University, Stanford, California
(Received April 13, 1956)

The charge distribution of the deuteron has been studied by electron-scattering experiments using 188-Mev and 400-Mev electrons. Both deuterated-polyethylene foils and deuterium gas targets were used. Two different scattering apparatuses were also used. All experiments are consistent with the following results.

The charge of the deuteron is extended over a larger volume than that inferred from low-energy neutron-proton scattering. Specifically, the effective range of the neutron-proton potential is found to be at least $(2.18\pm0.15)\times10^{-13}$ cm as compared with the *n-p* scattering result of $(1.70\pm0.03)\times10^{-13}$ cm. It is possible also to fit the data using a 1.70×10^{-13} cm effective range, and a deuteron consisting of a point neutron and a proton with an rms radius of $(0.82\pm0.17)\times10^{-13}$ cm. This procedure, however, violates the assumption of the charge independence of the internal structure of nucleons. Finally, the 1.70×10^{-13} cm effective range could be preserved by suitably modifying the Coulomb law at small distances.

I. INTRODUCTION

THE scattering of electrons from nuclei gives information about the distribution of charge in the nuclei.[1] Since the charge distribution (wave function) of the deuteron can be calculated directly from a knowledge of the potential between the neutron and the proton, an experimental measurement of this charge distribution by electron scattering would be expected to throw some light on the properties of the neutron-proton potential.

The effective range of this potential has been quite accurately determined from low-energy neutron-proton scattering experiments,[2] and, indeed, the analysis of these experiments is so fundamental and straightforward that it would be surprising if an electron-scattering experiment should give a different result. However, the low-energy, neutron-proton scattering experiments have not yet yielded information about the shape of the nuclear potential between the neutron and proton. It seemed worthwhile, therefore, to do the electron scattering experiment to discover whether any information about the potential shape could be obtained.

II. EXPERIMENTAL PROCEDURES

Scattering from the deuteron has been observed at electron beam energies of 188 Mev and 400 Mev by detecting the elastically-scattered electrons. The 188-Mev data were obtained with the scattering apparatus at the halfway station[3] of the Stanford Mark III linear accelerator. The 400-Mev scattering was performed in the end station of the same accelerator with a larger apparatus similar in principle to that at the halfway station. In addition, a check run at 188 Mev was made in the end station. The scattering was performed also with both solid (CD_2) and gas targets as before.[3] All runs at the two energies, at both stations, and with both kinds of targets are consistent with one another.

A schematic diagram of the end station installation is shown in Fig. 1. The electron beam from the accelerator is deflected and its spread in energy limited by the energy defining slit. A second deflection directs the beam through a secondary-emission monitor[4] and onto either the scattering foil or gas target. The gas target is a cylindrical tube $\frac{3}{4}$ in. in diameter and 8 in. long, with its axis along the beam. The gas pressure is about 2000 psi. The beam striking the target has a cross section of roughly $\frac{1}{4}$ in. by $\frac{1}{4}$ in. The scattered electrons are deflected upward and analyzed by a 36-in. 180° double-focusing magnet spectrometer and then detected by a Lucite Čerenkov counter 4 in. in diameter. A large platform mounted on the spectrometer carries 10 tons of lead and concrete shielding around the counter. The spectrometer and counter are mounted on a twin 5-in. gun mount supplied by the United States Navy; the entire apparatus can be rotated by remote control about the scattering target. The Faraday cup shown in Fig. 1 has not yet been installed.[5]

The 188-Mev data are essentially a more careful rerun of the data published earlier.[3] Improvement in the data results chiefly from better statistics, repeated measurements, and a better understanding of the effects associated with the use of thick targets with the double-focusing magnet spectrometer. Nevertheless, there is still a lack of reproducibility in the data possibly due to hysteresis effects and small drifts in the magnetic field of the magnets. Efforts are being made to install magnetic-field measuring devices to replace the method of deducing the magnetic field from the magnet current.

In the 188-Mev runs at the halfway station, elastic

* The research reported here was supported jointly by the Office of Naval Research and the U. S. Atomic Energy Commission and by the U. S. Air Force, through the Office of Scientific Research of the Air Research and Development Command.

[1] See, e.g., Hahn, Ravenhall, and Hofstadter, Phys. Rev. **101**, 1131 (1956) for recent measurements on large nuclei.

[2] See, e.g., J. M. Blatt and V. F. Weisskopf, *Theoretical Nuclear Physics* (John Wiley and Sons, Inc., New York, 1952), Chap. II.

[3] This apparatus is described in J. A. McIntyre and R. Hofstadter, Phys. Rev. **98**, 158 (1955).

[4] G. W. Tautfest and H. R. Fechter, Rev. Sci. Instr. **26**, 229 (1955).

[5] For details of this apparatus see E. E. Chambers and R. Hofstadter, Phys. Rev. **103**, 1454 (1956), this issue.

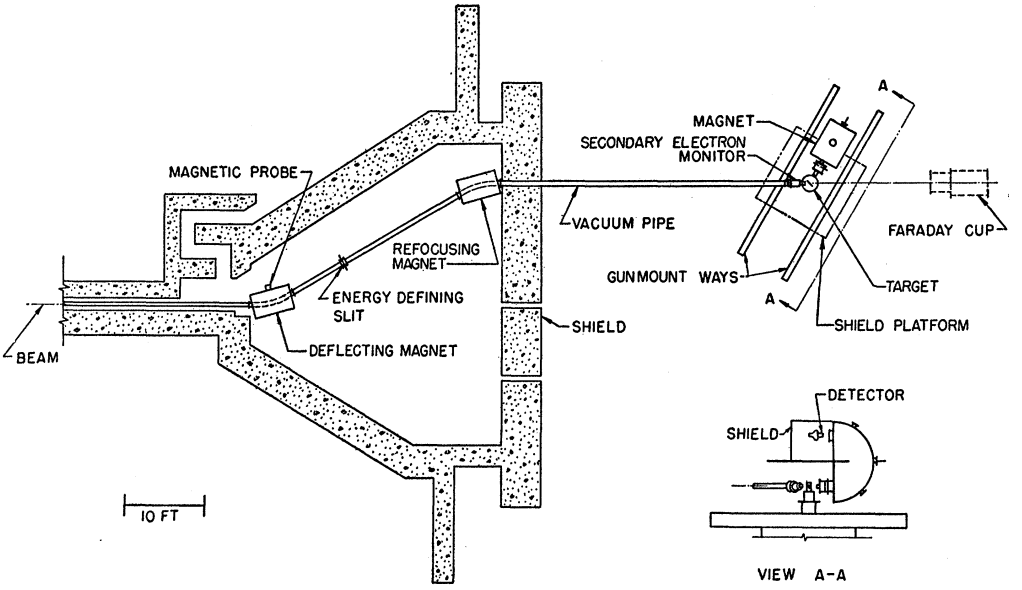

FIG. 1. Schematic diagram showing the end station electron-scattering apparatus.

scattering from the deuteron was observed at angles between 35° and 120°. Five runs were made with the solid target, one with the gas target. One 188-Mev run, covering six angles, also was made in the end station with the gas target. In all runs (except the one in the end station) scattering from the proton also was measured at 50° to give a reference point (using a corresponding solid or gaseous hydrogen target). In all, 36 points were taken at 188 Mev including the proton points.

The 400-Mev deuteron points at the end station were taken at 5° intervals between 30° and 60°. Six runs were made with the gas target, one with the solid target. A proton reference point was taken at 30° in each run. In all, 27 points were taken at 400 Mev including the proton points.

A typical curve, showing the number of 188-Mev electrons scattered by the solid target at 80°, is shown in Fig. 2. Figure 3 shows data at 60° using the gas target. The area between the CD_2 and carbon curves or under the gas curve is then measured to determine a quantity proportional to the number of elastically-scattered electrons at a particular angle. With curves such as these, and their associated areas, the cross sections for elastic scattering at the various angles and energies can be computed.

III. CORRECTIONS TO DATA

A number of corrections must be applied to the areas obtained from the curves such as the ones shown in Figs. 2 and 3. These corrections will now be considered.

1. When using the solid target, the normal to the target is rotated to one-half the scattering angle to equalize energy loss in the target. Thus, the target thickness is $t\sec(\theta/2)$, where t is the thickness normal to the target. With the gas target, on the other hand, the target thickness is $t'\csc\theta$, where t' is the length of the gas target "seen" by the electron counter through the spectrometer magnet.

2. Because of the recoil of the deuteron, the elastically scattered electrons at various angles have different energies. Since the exit-slit width of the spectrometer has a constant value of $\Delta p/p$ (p=electron momentum), the abscissa interval in Figs. 2 and 3 should be changed from dI (I=magnet current) to dp/p. Therefore, the areas obtained are multiplied by $(dp/p)\times(1/dI)=(1/p)\times(dB/dH)$, where dB/dH is the slope of the magnetization curve of the spectrometer (neglecting end effects). Because of the saturation of the halfway-station spectrometer and the significant recoil energy of the deuteron dB/dH varies by 60% for the range of angles

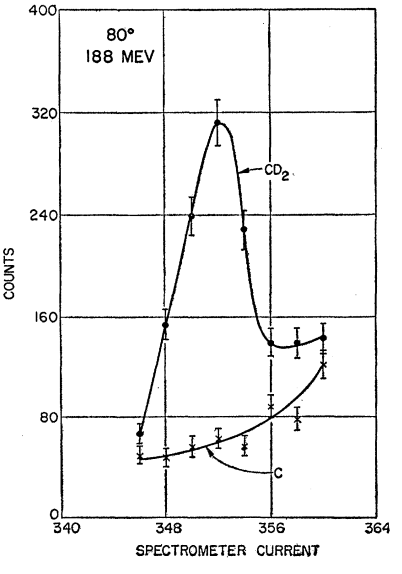

FIG. 2. Elastic electron-scattering data obtained at 80° using the solid CD_2 target. The scattering from a carbon target is shown by the lower curve. The electron beam energy is 188 Mev.

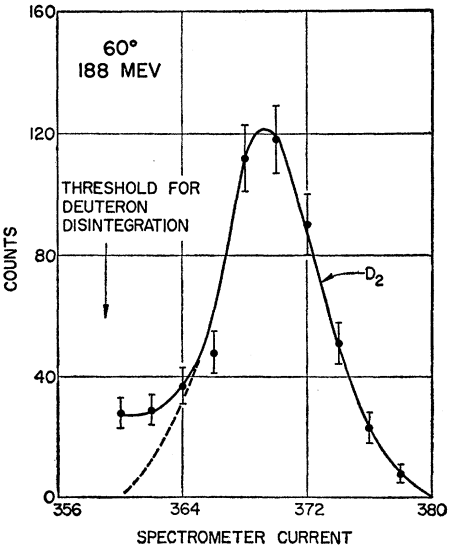

FIG. 3. Elastic electron-scattering data obtained at 60° using the gas target. The electron beam energy is 188 Mev. The points to the left of the dotted line represent electrons which have lost energy in the process of disintegrating the deuteron.

covered in the deuteron experiment. In the end station, dB/dH is constant for the 188-Mev scattering and varies by 15% for the 400-Mev scattering.

3. The number of electrons passing through the target during the counting period must be divided into the area measured under the scattered electron peaks. As mentioned before, the beam is monitored by a secondary-emission monitor. This type of monitor has been found to be stable within a few percent over long periods of time.[4]

4. The scattering cross sections are determined for each run by normalizing the corrected area associated with the hydrogen scattering to the cross section for proton scattering as determined by Chambers and Hofstadter.[5]

5. The radiative correction to the scattering theory[6] has been applied. This amounted to no more than 3% because of the method of normalizing to hydrogen.

6. Correction was made for electrons lost from the experiment due to bremsstrahlung in the target.[7] At most, this was a 3% correction.

IV. EXPERIMENTAL CHECKS

A number of checks was made to determine whether the corrections of the last section were valid. These checks were often not pushed beyond an accuracy of 10% even though better accuracy could have been obtained. This was because the experimental accuracy was already limited to 10% because of lack of reproducibility in the data as already mentioned in Sec. II. Following are the experimental checks made on the system.

1. The geometrical correction to the target thickness was checked in two ways: First, for scattering at 50°, the solid target was set at 25° and then at 55°. The counting rate varied as $\sec(\theta/2)$ as it should to within a factor of 3%. This result showed not only that the calibration of the target angle was correct but also that the counter beyond the spectrometer magnet could "see" all of the target area struck by the incoming electron beam. This latter conclusion follows from the fact that the horizontal dimension of this active target area depends on the target angle (in this test this dimension changed by 70%).

The second check on the target thickness follows from the agreement between the scattering from the solid and the gas targets. This agreement was on the average better than 5%. Variations among different solid-target runs was sometimes greater than this.

2. The value of dB/dH, the slope of the magnetization curve for the halfway-station spectrometer, was checked by four methods. The first method was to measure the magnetization curve at the center of the spectrometer with a Rawson rotating coil fluxmeter of 2% accuracy. The second method was to measure the voltage induced in a fixed coil when the spectrometer current was changed by a small amount. A ballistic galvanometer was used to measure this voltage. This measurement gave dB/dH directly. The third method was to determine B and H from the recoil energies measured in the hydrogen and deuterium scattering. At a given angle the energy of the scattered electron could be calculated and B was obtained from this energy value. H was obtained at that angle experimentally by noting the magnet current required to bend the scattered electrons through the spectrometer. This method thus determined the magnetization curve over the region used in the scattering experiments. Finally, the fourth method was to relate B and H by measuring the difference in spectrometer current readings between the elastically- and inelastically-scattered electrons from carbon nuclei. Since the nuclear energy levels of carbon are well known, this information provided a 10-Mev section of the magnetization curve at 188 Mev and at 150 Mev, the energies at which the carbon measurements were made. The last two methods measured more nearly the desired quantity as they include the effects of the fringing fields at the entrance and exit of the spectrometer. The four methods agreed with each other within 10%.

For the end-station spectrometer, a rough check of the magnetization curve was made with the Rawson flux meter. The curve used in processing the data, however, was determined from the spectrometer currents associated with the electrons scattered from hydrogen as measured by Chambers and Hofstadter.[5] The electrons scattered from deuterium checked this calibration within a few percent. Since the change in

[6] J. Schwinger, Phys. Rev. **76**, 790 (1949).
[7] H. A. Bethe and J. Ashkin, *Experimental Nuclear Physics*, edited by E. Segrè (John Wiley and Sons, Inc., New York, 1953), p. 272.

the slope is only 15% for the 400-Mev data and is zero for the 188-Mev data at the end station, the slope does not need to be known accurately at these energies.

3. A check was made on the constancy of the dispersion $\Delta p/p$ of the halfway-station spectrometer by placing a double slit at the spectrometer exit. The double peak resulting from the monoenergetic scattered electrons passing through these slits as the spectrometer current was varied gave the change in current required to move the electrons a fixed distance at the exit slit. A check at 186 Mev and at 143 Mev gave a 12% discrepancy. Because the spectrometer current shunt had been damaged and was found later to be in error by 10%, this discrepancy is not viewed seriously and is ignored in processing the data.

A check on the dispersion of the end-station spectrometer using film exposures indicates good agreement with the theory of the magnet. It is known also from film exposures that this spectrometer gives a small focused spot ($\frac{1}{4}$ in. by $\frac{1}{4}$ in.) at the exit slit when analyzing 400-Mev monoenergetic electrons.

4. An over-all check on spectrometer characteristics is provided by performing the 188-Mev scattering experiment at both the halfway station and the end station. Since the magnetization curve of the end-station magnet is linear at this energy, the agreement in scattering data obtained at these two locations gives an excellent check of all of the characteristics of the halfway-station spectrometer. This check provides another reason to doubt the 12% variation found in the dispersion of the halfway-station spectrometer. Finally, the agreement between the 400-Mev data in the end station and the 188-Mev data gives reason for confidence in the characteristics of the end-station spectrometer at 400 Mev. Chambers and Hofstadter[5] have also measured the magnetic field of the end-station spectrometer and its gradient over a wide range of energies and have found the values predicted by the magnet design.

5. The effect of the walls of the gas target has been checked by McAllister and Hofstadter[8] by placing a metal foil comparable in thickness to the target wall between the target and the spectrometer. No change in the area under the elastically scattered electron peaks (such as the peak in Fig. 2) was observed within the accuracy of the measurement (10%).

6. A plateau of Čerenkov-counter pulse heights was taken before each run to determine the discriminator setting of the counter-scaler combination. The counting system was also checked periodically by inserting a radioactive source and crystal in front of the Lucite Čerenkov counter which then acts as a light pipe.

7. There is some uncertainty involved in measuring the areas under the experimental peaks (see Fig. 3). This occurs because there are inelastically-scattered electrons (to the left of the peak) which have disintegrated the deuteron. These electrons must be rejected in the elastic-scattering measurement. Thus, the area is bounded on the left with the dotted line which has been sketched in to make the elastic peak roughly symmetrical. The accuracy of this procedure has been checked in two ways: The first is to sketch in dotted curves that seem to be in limiting possible reasonable positions. The area under the peak as measured by a planimeter is found to vary no more than $\pm 5\%$ for these changes. The second check is to change the abscissa and ordinate scales of the peaks obtained at the various angles so that the peaks will coincide with one another when they are superimposed.[9] The lower left portions of the peaks are ignored when making this superposition so that the problem of the inelastic scattering is circumvented. The abscissa and ordinate compression factors then give the ratios of the areas at the various angles. This procedure gave agreement with the other method of area measurement within $\pm 10\%$, the variations being on both sides of the first measurements. This shows that there is no large systematic error introduced by the inelastic electrons in measuring the area. This second procedure was not carried out very carefully as it was used only to detect a systematic error.

8. There is little doubt that the above checks, which gave 10% discrepancies, could have been refined to give better consistency. The effort was not made to carry out this refinement because the reproducibility of the data was not better than 10% even when all experimental parameters were held constant. As mentioned before, this lack of reproducibility is thought to be caused by drifts in the field of the beam-deflecting magnet before the energy-selecting slit or in the spectrometer magnet. For example, if a change in field of 0.1% should occur in either of these magnets while the point at current reading 374 in Fig. 3 was being taken, an error of 8% would occur in the number of counts obtained at that point. Such a change is thought to be not unlikely and would account for the 10% lack of reproducibility observed in the data.

V. HANDLING OF DATA

The data from each run were normalized by means of the experimental proton point. The deviation of the proton scattering from the scattering of a point proton has been determined by Chambers and Hofstadter[5] to be $(0.88\pm 0.05)\%$ at 50° and 188 Mev and $(0.81\pm 0.05)\%$ at 30° and 400 Mev. Using these deviation factors and the theoretical cross section for scattering from a point proton,[10] the proton scattering cross sections are found to be (omitting the radiative corrections):

$$188 \text{ Mev}, 50°, \quad \sigma = 3.23\times 10^{-30} \text{ cm}^2 \text{ sterad}^{-1},$$

$$400 \text{ Mev}, 30°, \quad \sigma = 5.39\times 10^{-30} \text{ cm}^2 \text{ sterad}^{-1}.$$

[8] R. W. McAllister and R. Hofstadter, Phys. Rev. **102**, 851 (1956).

[9] This method was suggested to the author by Professor J. F. Streib.

[10] M. N. Rosenbluth, Phys. Rev. **79**, 615 (1950).

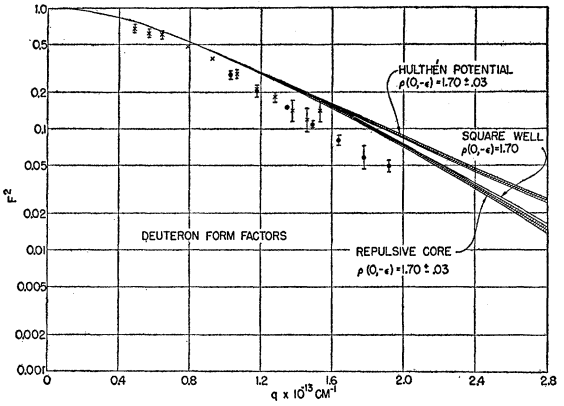

FIG. 4. Experimental points and theoretical F^2 (form factor)^2 curves. The three theoretical curves are for deuterons held together by three types of neutron-proton potentials. The shaded theoretical bands represent the uncertainty in the theoretical curves introduced by the standard deviation in the presently accepted effective range value of $(1.70\pm0.03)\times10^{-13}$ cm.

From these values and the experimental ratios between proton and deuteron scattering, cross sections were obtained for the deuteron points.

This method of determining the deuteron cross sections gives excessive weight to the proton point, however, as a poor proton point will result in all of the deuteron points in a given run being given incorrect cross sections. Consequently, a constant multiplying factor was applied to the cross sections of each run so as to give a least squares fit for all of the data. This adjustment did not change the normalization of any run by more than 2%.

The mean value for the cross section for each deuteron angle was then obtained by averaging the deuteron points from the various runs. The standard deviation of this mean was computed from the different cross-section values used in obtaining the mean. In almost all cases, the deviations between different runs were larger than the statistical deviations. At angles where only one run was made, the deviation was arbitrarily set equal to that for the neighboring angle since that deviation was always larger than the statistical one for the single run.

In order to compare the experimental results with theory, it is convenient to divide the experimental cross sections by the theoretical cross section for the scattering by a point particle with the mass and charge of the deuteron [see Eq. (4)]. This ratio is designated by F^2, (form factor)^2, and is plotted in Fig. 4 as a function of q, the momentum transfer of the scattered electron in the center-of-mass system. The theoretical curves plotted in Fig. 4 will be discussed in the next section.

VI. THEORETICAL CONSIDERATIONS

As mentioned before, there is a simple theory for the deuteron.[2] From low-energy neutron-proton scattering data, an effective range of the neutron-proton potential can be determined which is essentially independent of the shape of the potential. Using Bethe's notation,[11] the effective range of the triplet potential is found to be $\rho(0,-\epsilon)=(1.70\pm0.03)\times10^{-13}$ cm.[12] (ϵ is the binding energy of the deuteron.)

In the work which follows, three types of neutron-proton potentials have been considered: the Hulthén potential, $V(r)=e^{-Kr}/(1-e^{-Kr})$ (which is essentially a Yukawa potential but can be handled more easily mathematically),[13] the square-well potential, and a repulsive-core potential[14] yielding a deuteron wave function of the type

$$\psi=0 \text{ for } r<a, \quad \psi=(1/r)\{e^{-\alpha r}-e^{a(\gamma-\alpha)}e^{-\gamma r}\} \text{ for } r>a.$$

A deuteron binding energy of $\epsilon=2.226$ Mev is used.[15]

For the Hulthén potential, $\rho(-\epsilon,-\epsilon)$ is evaluated in terms of the wave function, $\rho(-\epsilon,-\epsilon)$ then being a function of K, the Hulthén potential parameter. To evaluate K, the value of $\rho(-\epsilon,-\epsilon)$ must be found from $\rho(0,-\epsilon)=1.70$.[16] This is done by combining Eqs. (33), (10), and (13a) from Bethe's article[11] to obtain

$$\rho(\epsilon_2,\epsilon_1)=r_0-2Pr_0^3(k_2^2+k_1^2). \tag{1}$$

For the Yukawa well, Blatt and Jackson[17] give P to be 0.14 so that Eq. (1) above gives $r_0=\rho(0,0)=1.63$ and $\rho(-\epsilon,-\epsilon)=1.77$. For this value of $\rho(-\epsilon,-\epsilon)$, K, the Hulthén potential parameter, is found to be 1.13. The wave function for the deuteron is then determined and also its square, the charge distribution. To obtain the charge distribution in the laboratory system, the lengths given above are divided by two. Using the Born approximation for electron scattering from this distribution,[18] the scattering is found to be[19]

$$F(q)=\frac{1.580}{q}\left(\tan^{-1}\frac{q}{0.930}-2\tan^{-1}\frac{q}{3.19}+\tan^{-1}\frac{q}{5.45}\right), \tag{2}$$

where $q=(2p/\hbar)\sin(\theta/2)[1+(2p/Mc)\sin^2(\theta/2)]^{-\frac{1}{2}}$, p is the incoming electron momentum, θ is the scattering angle in the laboratory, and M is the deuteron rest mass. $F^2(q)$ is defined as the ratio of actual scattering to that expected from a point scatterer. Equation (2) thus gives the theoretically expected modification to point-charge scattering of a deuteron bound together by a Hulthén potential.

Electron scattering from a deuteron with a square-

[11] H. A. Bethe, Phys. Rev. **76**, 38 (1949).
[12] See reference 2, p. 85.
[13] L. Hulthén, Arkiv Mat. Astron. Fysik. **28A**, No. 5 (1942).
[14] V. Z. Jankus, Phys. Rev. **102**, 1586 (1956).
[15] See reference 2, p. 51.
[16] Henceforth, all lengths will be expressed in units of 10^{-13} cm.
[17] J. M. Blatt and J. D. Jackson, Phys. Rev. **76**, 18 (1949).
[18] W. A. McKinley, Jr. and H. Feshbach [Phys. Rev. **74**, 1759 (1948)] have shown that the Born approximation is accurate to better than ½% for scattering from singly-charged particles.
[19] See, e.g., M. E. Rose, Phys. Rev. **73**, 279 (1948), for calculation of form factors.

well potential between neutron and proton has been calculated by Smith.[20] A procedure similar to that used with the Hulthén potential was followed to determine the range and depth of the square well for use in Smith's equation. By using the data in Blatt and Jackson[17] as above, $\rho(0,0)$ was found to be 1.73 for $\rho(0,-\epsilon)=1.70$. The potential range to give this value for $\rho(0,0)$ was found to be 2.04 with a potential depth of 35.2 Mev. Smith's equation then gives the form factor $F(q)$ for scattering from such a deuteron.

Jankus[14] has calculated the scattering from a repulsive-core potential using the repulsive-core wavefunction given above. If one investigates instead an extreme repulsive-core model [$\psi=(1/r)e^{-\alpha r}$ beyond the core radius], it may be shown that $\rho(-\epsilon,-\epsilon)=1.67$ for $\rho(0,-\epsilon)=1.70$. The assumption has been made in the following that this is true for Jankus' wave function also. Therefore, the repulsive-core scattering in this paper has been calculated for $\rho(-\epsilon,-\epsilon)=1.67$. A core radius of 0.65 has been used.

The values for $F^2(q)$ are plotted in Fig. 4 for the Hulthén, the square-well, and the repulsive-core deuterons. The 0.03 standard deviation in the effective range value is indicated for the Hulthén and repulsive-core potential by the shaded areas.

Thus far, the deuteron has been considered as consisting solely of a neutral and a charged particle attracted to each other by a central potential and in an S state. The magnetic moments of the neutron and proton and the mixture of D state in the wave function must also be considered as to how they affect the electron scattering. The magnitude of these effects has been investigated by Jankus.[14] He has found that the scattering of electrons from the magnetic moment of the deuteron has a cross section

$$\sigma_{\text{mom}}=\{\tfrac{2}{3}(e^2/Mc^2)^2\mu_D^2[1+\csc^2(\theta/2)]\}\times\{1+(2p/Mc)\sin^2(\theta/2)\}^{-2}\times F_{\text{mom}}^2(q)=\sigma_{\text{point mom}}\times F_{\text{mom}}^2(q), \quad (3)$$

where e is the electronic charge and μ_D is the magnetic moment of the deuteron in nuclear magnetons. This is seen to be negligible, in most cases, when compared to the scattering from the charge of the deuteron which is simply $F_{\text{charge}}^2(q)$ times the Mott scattering from a point charge[21]:

$$\sigma_{\text{charge}}=\left(\frac{e^2}{2pc}\right)^2\csc^4(\theta/2)\cos^2(\theta/2)\times\{1+(2p/Mc)\sin^2(\theta/2)\}^{-1}\times F_{\text{charge}}^2(q)=\sigma_{\text{point charge}}\times F_{\text{charge}}^2(q). \quad (4)$$

For instance, at the largest scattering angle of 120° at 188 Mev, $\sigma_{\text{point mom}}/\sigma_{\text{point charge}}$ is 11% while at 90° it is only 3%. For the 400-Mev scattering at the largest angle, it is 4%.

The small admixture of D state in the deuteron wave function (about 4% of the charge distribution) affects the wave function in two ways: it contributes to the spherically symmetric part of the wave function, and it accounts for the quadrupole moment. The contribution to the electron scattering of these two D-state effects is shown by Jankus[14] to be of the order of no more than a few percent.[22]

Because of the smallness of all of the contributions to the cross section in comparison to the scattering from the charge, it is necessary in the following to consider only the charge scattering. Therefore, the experimental cross sections have been divided by the scattering from a point charge [$\sigma_{\text{point charge}}$ in Eq. (4)] to give the experimental F^2 plotted in Fig. 4 (see Sec. V).

VII. DISCUSSION OF RESULTS

Figure 4 shows that there is a large discrepancy between the theoretical curves and the experimental data. The following possibilities are available to explain this discrepancy:

1. The neglected factors mentioned in the last section should be taken into account. However, these factors all add to the theoretical curve and, hence, make the discrepancy in Fig. 4 larger. Thus, the discrepancy in Fig. 4 results. This feature of the deuteron scattering greatly simplifies the interpretation of the experimental results.

2. The experimental points may be made to agree with theory by increasing the effective range of the neutron-proton potential in the deuteron. If this is done a fit may be obtained for the data as shown in Figs. 5 and 6. For the Hulthén deuteron $\rho(0,-\epsilon)=2.47_{-0.32}^{+0.20}$, and for the repulsive-core deuteron $\rho(0,-\epsilon)=2.18\pm0.15$. The square-well deuteron is in-

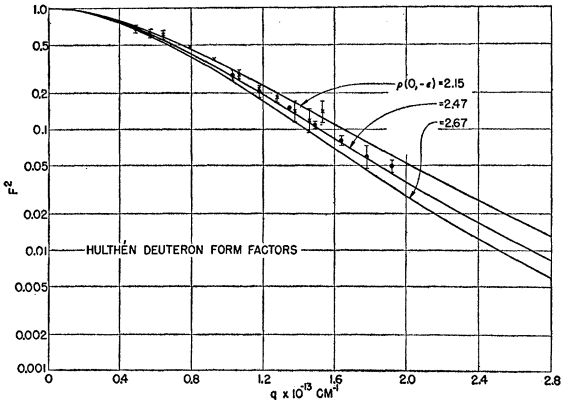

FIG. 5. Experimental points fitted by a theoretical Hulthén deuteron with suitable effective range. The upper and lower curves represent the extremes in effective range values that will still fit the experimental data.

[20] J. H. Smith, Ph.D. dissertation, Cornell University, 1951 (unpublished).

[21] N. F. Mott, Proc. Roy. Soc. (London) **A135**, 429 (1932).

[22] The effect of the D-state admixture was first calculated by L. I. Schiff, Phys. Rev. **92**, 988 (1953).

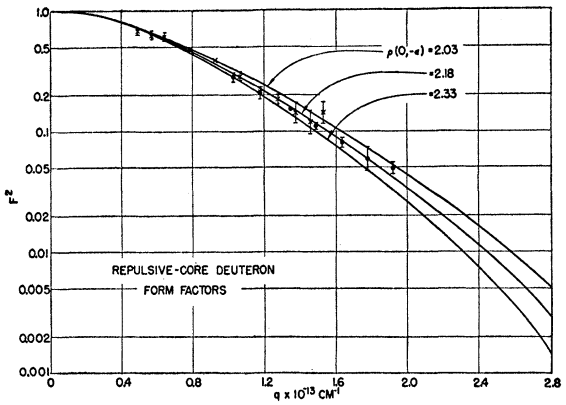

FIG. 6. Experimental points fitted by a theoretical repulsive-core deuteron with suitable effective range. The upper and lower curves represent the extremes in effective range values that will still fit the experimental data.

distinguishable from the repulsive-core deuteron (see, e.g., Fig. 4).

These effective range values are seen to be at least (16±5) standard deviations outside the presently accepted value for the effective range of 1.70±0.03. This latter value for the effective range is based on the simplest assumptions about the neutron-proton potential.[2] It is thus necessary to make a fundamental modification in the present ideas about nuclear forces in order to increase the effective range obtained by low-energy neutron-proton scattering a sufficient amount to agree with the results of the electron-scattering experiments.

3. An agreement between experiment and theory can be obtained by assuming that the charge cloud of the proton in the deuteron is spread out over a root-mean-square radius of about 0.8, while the cloud for the neutron extends over a region much smaller than this. This assumption is in agreement with the electron-proton scattering experiments of Chambers and Hofstadter[5] and the neutron-electron scattering experiments of Melkonian *et al.*[23] and Hughes *et al.*[24,25]

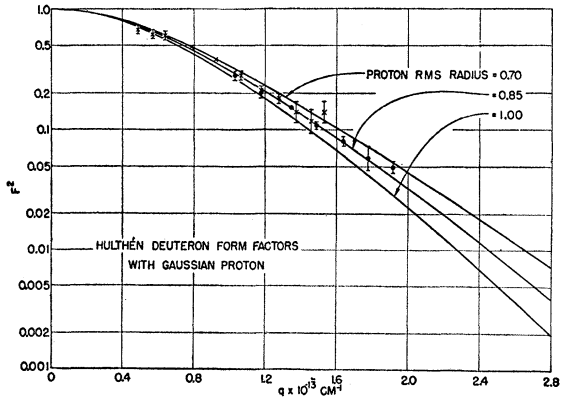

FIG. 7. Experimental points fitted by a theoretical Hulthén deuteron containing a proton with suitably spread-out charge distribution. The radial dependence of the proton charge density is Gaussian.

The form factor of a deuteron which contains a proton with form factor F_P is $F_P \times F_D$, where F_D is the usual deuteron form factor. Figure 7 shows the modified deuteron form factor for a Hulthén deuteron which contains a proton with Gaussian radial charge distribution. The best fit with the experimental data is obtained with a proton rms radius of 0.85. The upper and lower limit proton radius values are 1.00 and 0.70, respectively. Figure 8 shows the repulsive-core deuteron form factor modified by a Gaussian proton. The curves here fit for a proton rms radius of 0.80±0.15.

Some change in these values occurs if the proton radial charge distribution is different from the Gaussian. The change is such as to increase the proton rms radius values required to fit the experimental data. Thus, the proton rms radius values of 0.85±0.15 for the Hulthén deuteron and 0.80±0.15 for the repulsive-core deuteron are minimum values. As mentioned above, the square-well deuteron gives the same result as the repulsive-core deuteron.

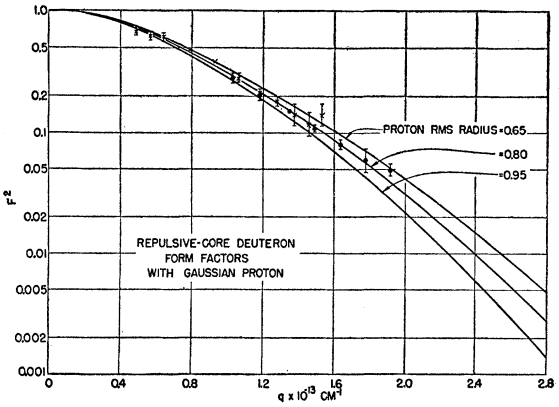

FIG. 8. Experimental points fitted by a theoretical repulsive-core deuteron containing a proton with suitably spread-out charge distribution. The radial dependence of the proton charge density is Gaussian.

Yennie[26] has pointed out that the assumption made here of a proton and neutron of different size existing in the deuteron is almost equivalent to abandoning the property of the charge independence of the internal structure of nucleons. His argument is that, if one assumes charge independence of the neutron and proton in the deuteron, the π^- meson cloud about the neutron and the π^+ meson cloud about the proton will just

[23] Melkonian, Rustad, and Havens, Bull. Am. Phys. Soc. Ser. II, 1, 62 (1956).

[24] Hughes, Harvey, Goldberg, and Stafne, Phys. Rev. **90**, 407 (1953).

[25] For a discussion of the relation between the neutron-electron interaction and the extension of the neutron charge cloud, see, e.g., H. A. Bethe and F. de Hoffmann, *Mesons and Fields* (Row, Peterson, and Company, Evanston, 1955), Vol. 2, pp. 297–299.

[26] D. R. Yennie, Phys. Rev. **100**, 1795 (1955) and Yennie, Lévy, and Ravenhall (to be published).

cancel each other because the wave function for the neutron in the deuteron is the same as that for the proton. Thus, the protonic nucleon core is alone responsible for the charge distribution of the deuteron as measured by the electron-scattering experiments. This argument applies also to the mesons exchanged between the neutron and proton. Therefore, either the nucleon core has an rms radius of 0.8 or the assumption of charge independence is invalid. Since the nucleon Compton wavelength is 0.2, the first possibility seems unlikely. Therefore, it seems necessary to abandon the assumption of charge independence of nucleons if the discrepancy of Fig. 4 is to be removed by postulating a proton rms radius of 0.8 and a smaller neutron in the deuteron.

4. The discrepancy between theory and experiment in Fig. 4 can be removed by assuming a modification of the Coulomb law of interaction between the deuteron and the scattered electrons.[26] This follows from the fact that an electron-scattering experiment measures the potential of the scatterer. A departure of this potential from the Coulomb law has heretofore been interpreted as evidence for a spread-out charge distribution. However, if the Coulomb potential itself is not the correct one at small distances for a point charge, then a different charge distribution would be implied by the electron-scattering experiments. Thus, a suitable modification of the Coulomb potential can be invoked to obtain agreement between experiment and theory in Fig. 4.

VIII. CONCLUSIONS

There is a discrepancy between the charge distribution of the deuteron as determined by the electron-scattering experiments reported here and the charge distribution as inferred from low-energy neutron-proton scattering. This discrepancy is associated only with the charge of the S state of the deuteron. In order to remove the discrepancy, the following three procedures are possible:

1. Increase the effective range of the neutron-proton potential from the presently accepted value of $(1.70\pm0.03)\times10^{-13}$ cm to at least $(2.18\pm0.15)\times10^{-13}$ cm. This latter value is 16 ± 5 standard deviations higher than the present value. This procedure entails a re-evaluation of the fundamental nuclear theory used in obtaining the effective range from low-energy neutron-proton scattering experiments.

2. Postulate a point neutron and a proton with rms radius $(0.83\pm0.17)\times10^{-13}$ cm as the components of the deuteron. This procedure entails the abandonment of the assumption of the charge independence of the internal structure of nucleons.

3. Assume that the Coulomb law of interaction between the scattered electron and the deuteron is modified at small distances.

Finally, it should be noted that because of the uncertainty in interpreting the experiments, no information can be deduced concerning the shape of the neutron-proton potential.

IX. ACKNOWLEDGMENTS

The author is greatly indebted to Professor Robert Hofstadter, who has conceived and supervised the electron-scattering program at Stanford, for many fruitful discussions and for his continued interest in this problem. Professor D. R. Yennie and Dr. D. G. Ravenhall have been very kind in making clear the theoretical implications of the experiment. Miss Sobhana Dhar has helped greatly in the later stages of taking data and is responsible for a number of the calculations. The author also wishes to thank Mr. V. Z. Jankus for making his deuteron-scattering calculations available as they were obtained, E. E. Chambers, R. W. McAllister, J. H. Fregeau, and B. R. Chambers for information and assistance on experimental problems and Mrs. K. R. Machein for calculating many of the theoretical curves.

The new end-station facilities are the result of the cooperation of many people: Professor R. Hofstadter and Mr. E. L. Rogers designed the magnet spectrometer; Mr. B. Smith of the San Francisco Naval Shipyard supervised the conversion of the gun mount; F. W. Bunker and J. H. Fregeau were responsible for its installation; B. R. Chambers designed and supervised the construction and assembly of the remaining structural components of the system; L. H. Franklin designed and supervised the installation of the electrical system, and E. E. Chambers designed the counting assembly and was responsible for putting the entire system into operation.

Finally, the author thanks the accelerator crew, under the direction of Professor R. F. Mozley, whose efforts have made this experiment possible.